

MODIFIED KT-DIAGRAM FOR STRESS RAISER-INVOLVED FATIGUE STRENGTH ASSESSMENT

O. M. Herasymchuk

UDC 539.4

The model for evaluating the fatigue strength of specimens and structure elements with sharp-edged and deep stress raisers (notches) or defects, which can be treated as initial cracks, is advanced. The model is based on the modification of known fracture mechanics approaches with employing the modified Kitagawa–Takahashi diagram. The model starts from the fact that cyclic loading of sharp-edged notch-containing specimens over the nominal stress span below the endurance limit of smooth specimens results in a crack penetrating to a certain size from the root of the notch, with its further arrest due to the two basic factors: descending gradient of local stresses ahead of the notch root and gradually growing effect of crack closure behind its tip. The crack size is dependent on the stress span and notch depth. The model permits of calculating the boundary curve of threshold stress spans and corresponding tolerable crack sizes for a sharp-edged notch of any depth, using only the characteristics of static strength and microstructure of the initial material. The model reliability was verified with experimental results taken from the literature, the calculation and experiment were in good agreement. The model need not long-term and labor-consuming fatigue and fatigue crack resistance tests to get parameters necessary for the model implementation. The model calculations would require only the data on static strength characteristics (elastic modulus, Poisson's ratio, and proportionality limit), obtained from short-time tensile tests of standard specimens from an examined material, and microstructure characteristics (grain size, Taylor factor, and Burgers vector), determined from microstructure analysis of the initial material.

Keywords: fatigue strength, stress raisers (notches), boundary curve of threshold stress spans, KT-diagram, fatigue crack.

Notation

- b – Burgers vector (\vec{b}) module
 d – grain size, maximum size of a microstructurally short crack
 D – notch depth
 E – elastic modulus
 h – spacing between neighboring parallel slip planes in the crystal lattice
 ΔK_{th} – threshold stress intensity factor span
 $\Delta K_{th,d}$ – threshold stress intensity factor span for a microstructurally short crack d deep
 $\Delta K_{th,eff}$ – effective threshold stress intensity factor span
 $\Delta K_{th,LC}$ – threshold stress intensity factor span for long cracks

Pisarenko Institute of Problems of Strength, National Academy of Sciences of Ukraine, Kyiv, Ukraine.
Translated from Problemy Prochnosti, No. 4, pp. 114 – 127, July – August, 2018. Original article submitted January 31, 2018.

K	– stress intensity factor
K_f	– effective stress concentration factor
K_t	– theoretical stress concentration factor
$K_{th,d}, K_{th,LC}$	– threshold stress intensity factors in terms of the load cycle maximum
l	– crack size (depth)
l_c	– critical distance parameter, material characteristic, which describes the surface layer depth with mechanical properties differing from those of the rest of the material
l_D	– size additional to the short crack size in the El Haddad equation
l_s	– material characteristic, which describes the depth of a physically small crack on the change in its propagation mechanism at a stress level maximally close to the endurance limit of smooth specimens
M	– Taylor factor
R	– stress ratio
r_p	– cyclic plastic region size
Y	– geometrical factor (stress intensity factor correction)
Y_1	– geometrical factor in the deepest point of the half-penny front of the plane surface crack against M
Y_2	– geometrical factor in the deepest point of the half-penny front of the plane surface crack perpendicular to the direction of applied tensile stress
ν	– Poisson's ratio
ρ	– notch root radius, crack tip radius
$\Delta\sigma$	– cycle stress span
$\Delta\sigma_e$	– endurance limit of smooth specimens in terms of the stress span
$\Delta\sigma_R$	– endurance limit at R in terms of the stress span
$\Delta\sigma_{th}$	– threshold stress span in the presence of a crack
σ	– tensile stress
σ_e	– endurance limit of smooth specimens in terms of the maximum cycle stress
σ_f	– internal friction stress in the crystal lattice
$\sigma_{max}, \sigma_{min}$	– maximum and minimum cycle stresses
$\sigma_{max,R}$	– endurance limit at R in terms of the maximum cycle stress
σ_p	– proportionality limit
σ_{-1}	– endurance limit under symmetrical cycling (amplitude or maximum cycle stresses)
$\sigma_{-1,e}$	– endurance limit of smooth specimens under symmetrical cycling (amplitude or maximum cycle stresses)
$\sigma_{0.2}$	– yield stress at 0.2% strain (yield limit)
σ_{nom}	– nominal stress
σ_{peak}	– maximum (peak) local stress at the notch root for the elastic distribution of local stresses
σ_{th}	– threshold stress in the presence of a crack
$\sigma_{th,max}, \sigma_{th,min}$	– maximum and minimum endurance limits for a sharp-edged stress notch

Introduction. Machine elements operating at variable loads experience fatigue damages that can lead to the nucleation of fatigue cracks, their propagation, and at last to failure. As a rule, the nucleation of fatigue cracks takes place at the stress concentration sites, determined both by the component construction (holes, fillets, slots, sharp ribs, etc.) and process engineering defects of the material (inclusions, undissolved precipitates, pores, microcracks, etc.) for component manufacturing or in-service defects (dents, scratches, corrosion cracks, etc.). Fatigue strength analysis of specimens and structure elements with stress raisers (notches) relies on different approaches depending on the notch geometry [1–5]. What those approaches have in common is the postulate that the fatigue strength of notch-containing specimens is governed by a minimum local stress necessary for the initiation of a fatigue crack near the notch root, which equals the endurance limit of smooth specimens. At the same time, for the notches of several types (sharp-edged and deep), the fatigue strength can be dependent on the threshold span of applied stress, which initiates the fatigue crack near the notch root that penetrates to a certain size and ceases its further propagation due to the two basic factors: descending gradient of local stresses from the notch root and gradually growing effect of crack closure (partial closure of edges behind the crack tip).

The above postulate is well illustrated by Fig. 1b where the classical relation of the threshold span of nominal stresses $\Delta\sigma_{th}$ against theoretical stress concentration factor K_t (Fig. 1a) is presented as the maximum (peak) local stress span near the notch root $K_t\Delta\sigma_{th}$ vs K_t [6]. As is seen, minimum stresses necessary for the initiation of a fatigue crack near the notch root at different K_t are at the same level, corresponding to the endurance limit of smooth specimens.

An ingenious approach was proposed in [7] where the critical distance concept was applied to analyze the fatigue strength of specimens with blunt and shallow notches ($K_t \leq 4$) using the characteristics of static strength and microstructure of the initial material. The critical distance is the interval from the notch root (in the direction perpendicular to the applied normal stress) where the span of local stresses reaches the endurance limit of smooth specimens during the action of nominal stresses, equal to the endurance limit of notch-containing specimens. This approach suggests that specimens with notches of this type behave similar to smooth specimens at their endurance limit. In other words, if in the smooth specimens at their endurance limit the cracks can appear whose size does not exceed the grain size d , i.e., microstructurally short cracks (MSC), as is stated, e.g., in [8], in the specimens with blunt and shallow notches at their endurance limit, the cracks of the same size can originate that do not further propagate. Just this behavior is illustrated by Fig. 1a at $K_t \leq 4$. Thus, such an approach defines the so-called endurance limit for the MSC initiation, and its evaluation would require the critical distance and equation for the curve of local stress distribution from the blunt notch root.

For sharp-edged and deep notches ($K_t > 4$), many researchers propose the approaches to fatigue strength analysis based on the Kitagawa–Takahashi diagram (KT-diagram) [9]. The KT-diagram is a powerful tool of fracture mechanics, which is widely used for the reliability and service life prediction of structure elements with crack-like defects. This diagram (Fig. 2a) depicts the two boundary (threshold) fatigue criteria: threshold stress for fatigue fracture, i.e., the endurance limit of a smooth specimen with small crack sizes and threshold stress intensity factor (SIF) span for the growth of a fatigue crack of larger sizes. Such an approach provides the basis for correlation between the traditional evaluation of fatigue life by the fatigue curve and its estimation built on fracture mechanics by the permissible damage concept, i.e., permissible crack sizes.

Authors [9] believed that the arrest of a surface fatigue crack was defined by the constant threshold SIF value for the cracks larger than ~ 0.5 mm. Below this size, the transition takes place at which the stress that equals the endurance limit of smooth specimens is more likely than threshold SIF to be the critical condition for the propagation of very small crack-like defects. Later in [10], the boundary curve equation for the threshold stress spans $\Delta\sigma_{th}$ (Fig. 2b, curve 1) was proposed that represents this gradual transition, using the additional fictitious/intrinsic size l_D to the crack size l as follows:

$$\Delta\sigma_{th} = \Delta K_{th,LC} / (Y \sqrt{\pi(l + l_D)}). \quad (1)$$

Here l_D is calculated by the formula

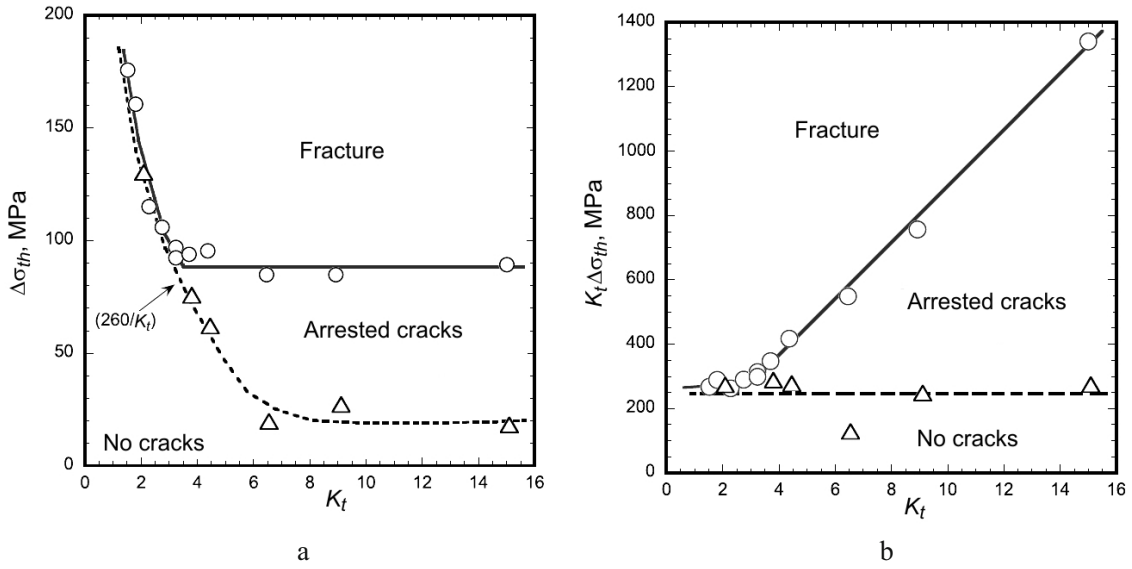


Fig. 1. Threshold span of nominal stresses $\Delta\sigma_{th}$ (a) and threshold span of maximum (peak) local stresses at the notch root $K_t\Delta\sigma_u$ (b) vs theoretical stress intensity factor K_t [6].

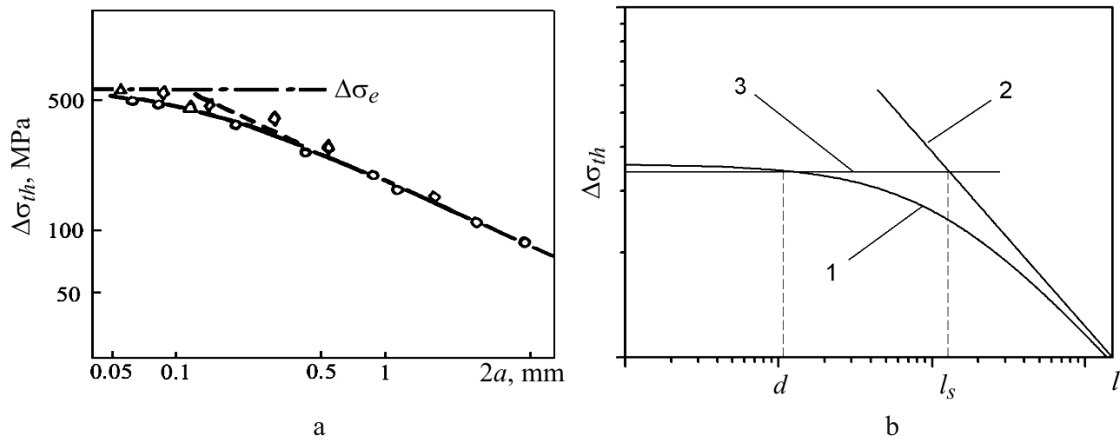


Fig. 2. KT-diagram: (a) Kitagawa–Takahashi experimental results [9]; (b) schematic KT-diagram [11] [(1) plot of Eq. (1), (2) plot of Eq. (3), and (3) plot of the equation $\Delta\sigma_{th} = \Delta\sigma_e$].

$$l_D = \frac{1}{\pi} \left(\frac{\Delta K_{th,LC}}{Y\Delta\sigma_e} \right)^2, \quad (2)$$

where $\Delta K_{th,LC}$ is the threshold SIF span for long cracks (LC), which characterizes their minimum motive force, $\Delta\sigma_e$ is the endurance limit of smooth specimens, and Y is the geometrical factor for the crack. The region on the diagram under curve 1 is the domain of arrested cracks (Fig. 2b).

The boundary curve for LC (Fig. 2b, curve 2) is described by the following equation:

$$\Delta\sigma_{th} = \Delta K_{th,LC} / (Y\sqrt{\pi l}). \quad (3)$$

Horizontal line 3 (Fig. 2b) defines the endurance limit of smooth specimens, which is described by the equation $\Delta\sigma_{th} = \Delta\sigma_e$. In the correct construction of the diagram [11], boundary curve 1 intersects line 3 at $x = d$, pointing to the presence of the crack of just this size at the endurance limit of smooth specimens.

The object of the present study is the application of the modified KT-diagram to the assessment of the fatigue strength of specimens and structure elements with deep and sharp-edged stress notches. Modification of known approaches [8, 12] resulted in the model, which can be used to calculate the boundary curve of threshold stress spans and corresponding admissible crack sizes for the notches of any depth, only with the characteristics of static strength and microstructure of the initial material. Reliability of the advanced model was verified with experimental results taken from the literature.

Model Construction. As experimental results of many researchers demonstrate [2, 8, 12], the threshold stress spans for physically small cracks (PSC) can be much smaller than those calculated by Eq. (1). It is determined by the incompletely evolved closure of PSC edges in contrast to LC. Thus, Eq. (1) provides the nonconservative prediction for PSC. In [8], the model for calculating $\Delta\sigma_{th}$ was advanced where an increase in the crack closure level with its size is accounted for after the exponential law, hence the KT-diagram is modified

$$\Delta\sigma_{th} = \frac{\Delta K_{th,d} + (\Delta K_{th,LC} - \Delta K_{th,d})(1 - e^{-k(l-d)})}{Y\sqrt{\pi l}} \quad \text{at } l \geq d, \quad (4)$$

where $\Delta K_{th,d}$ is the threshold SIF span for MSC of the d size

$$\Delta K_{th,d} = \Delta\sigma_e Y \sqrt{\pi d}, \quad (5)$$

k is the parameter that defines the crack closure evolution

$$k = \frac{\Delta K_{th,d}}{4d(\Delta K_{th,LC} - \Delta K_{th,d})}. \quad (6)$$

The expression in the numerator of Eq. (4) is the approximation of the so-called fatigue crack resistance curve, or simply the resistance curve (R -curve), and the coefficient of d in Eq. (6) is the fitting one. In [8], it was suggested that coefficient 4 gave the best agreement between the calculation by Eq. (4) and experimental data for examined materials. The boundary curve constructed in the logarithmical coordinates by Eq. (4) is depicted in Fig. 3 (curve 4). As is seen, boundary curve 4 also intersects horizontal line 3 at $x = d$, and for LC, it is consistent with boundary curves 1 {Eq. (1) [10]} and 2. In the PSC range, curve 4 narrows down the region of arrested cracks, as compared to curve 1. Thus, the threshold stress span $\Delta\sigma_{th}$ defined for PSC by model (4) [8] would require experimental evaluation of the material characteristics $\Delta\sigma_e$, $\Delta K_{th,LC}$, and d .

However, model (4) [8] does not take account of the initial defect (or sharp-edged notch) effect, giving rise to the crack penetration under cyclic loading below the endurance limit of smooth specimens. As is shown in [2], the region of arrested cracks narrows down considerably with the depth of such a defect. This effect is considered in the model proposed in [12]. The equation for calculating the boundary curve against the notch depth takes on the following form [12]:

$$\Delta\sigma_{th} = \frac{\Delta K_{th,eff} + (\Delta K_{th,LC} - \Delta K_{th,eff}) \left[1 - \sum_{i=1}^n v_i \exp(-l/l_i) \right]}{Y \sqrt{\pi(D+l)}}, \quad (7)$$

where $\Delta K_{th,eff}$ is the effective $\Delta K_{th,LC}$ value (i.e., without account of crack closure), which characterizes the maximum material resistance to crack propagation, l is the crack size from the notch root, Y is the geometrical factor for a crack-like notch, l_i is the crack portion where a certain mechanism of its closure prevails, and v_i is the weight percent. The parameters v_i and l_i are the fitting ones.

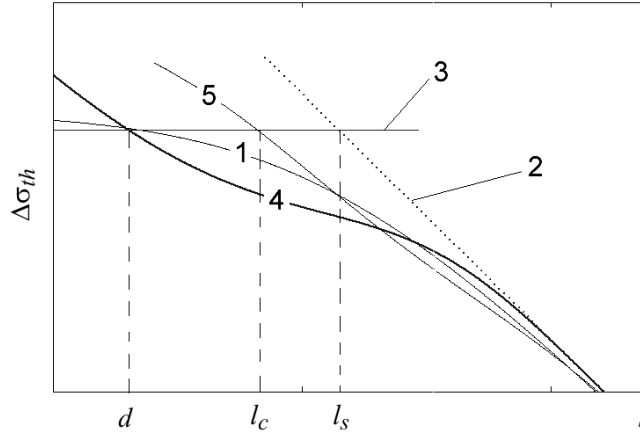


Fig. 3. Modified KT-diagram: (1) boundary curve by Eq. (1), (2) boundary curve for LC by Eq. (3), (3) plot of the equation $\Delta\sigma_{th} = \Delta\sigma_e$, (4) boundary curve by Eq. (4) [8], and (5) boundary curve by Eq. (7).

In [12], the sharp-edged notch is thought of as a crack of the D size whose edges do not close under cyclic loading. Therefore, the threshold SIF span for such a crack equals its effective value $\Delta K_{th,eff}$. As in Eq. (4), the expression in the numerator of Eq. (7) is the approximation of the resistance curve. The calculation by model (7) would require the experimental resistance curve in the $\Delta K_{th} - l$ coordinates, used for determining all necessary parameters.

One should distinguish between $\Delta K_{th,d}$ from Eq. (4) and $\Delta K_{th,eff}$ from Eq. (7), though they characterize the same value in those equations, only from different points of view. If the $\Delta\sigma_{th}(l)$ plot is constructed by Eq. (7) at $D = 0$, it would intersect the horizontal line $\Delta\sigma_{th}(l) = \Delta\sigma_e$ at $x = l_c$, which is other than d (Fig. 3, curve 5). Thus, it may be understood that the arrested crack of the l_c size exists at the endurance limit of smooth specimens, which it is not. This difference is due to different approaches to the description of the behavior of short cracks.

Thus, in determining SIF of a short crack $\Delta K_{th,d}$, Eq. (5) is used as for the long one, without account of the fact that the plastic region ahead of the crack tip is comparable with its size [8]. Therefore, $\Delta K_{th,d}$ does not correspond to the true value of threshold SIF for the short crack of the d size, which should equal $\Delta K_{th,eff}$ since the closure effect for such a crack is still nonexistent. So, in this case, we have the true crack size but fictitious threshold SIF at the endurance limit of smooth specimens.

In the other case, the expression to evaluate the threshold SIF $\Delta K_{th,eff}$ for the short crack of the d size can be written with the Dagdale correction for the plasticity of short cracks [13]

$$\Delta K_{th,eff} = (2\sqrt{\pi r_e F} + Y\sqrt{\pi d F})\sigma_e, \quad (8)$$

where F is the Dagdale correction for plasticity

$$F = \frac{1}{2} \left[\sec \left(\frac{\pi \sigma_e}{2\sigma_Y} \right) + 1 \right], \quad (9)$$

d is the linear crack size (dF is the linear crack size with the plastic region r_p ahead of the crack tip contrary to SIF for long cracks $K = Y\sigma\sqrt{\pi l}$, where l is the linear crack size with the plastic region r_p ahead of its tip since in this case $r_p \ll d$), σ_Y is the yield stress (proportionality limit σ_p or yield limit $\sigma_{0.2}$ may be used), σ_e is the endurance limit of smooth specimens in terms of a maximum cycle stress, r_e is the distance ahead of the crack tip along which the local maximum stress is considered constant $r_e = \rho/8$, where ρ is the crack tip radius.

Equation (8) can be rewritten as follows:

$$\Delta K_{th,eff} = \sqrt{l_c} \sigma_e. \quad (10)$$

The identity of Eqs. (8) and (10) can be easily verified if there are experimental data on $\Delta K_{th,eff}$, σ_e , σ_Y , and d , and ρ is taken to be $0.06d$ for an isotropic material or $0.03d$ for a strongly textured one [14]. Thus, the size l_c is a fictitious value. So, in this case [Eq. (7)], we have the true value of threshold SIF for MSC, with the fictitious short crack size at the endurance limit of smooth specimens.

The disadvantages of the above models for fatigue strength prediction are the use of fitting parameters and the necessity of performing additional experiments to evaluate the parameters of Eqs. (4) and (7).

Here the model is advanced that is the modification of models (4) and (7) in combination with an earlier suggested model of PSC growth [15]. The model can be applied to evaluating the fatigue strength of specimens and structure elements, which contain deep and sharp-edged stress notches or surface defects that can be presented as initial cracks. The equation of the boundary curve for threshold stresses in terms of a maximum cycle stress under symmetrical cycling for the notch D deep is set forward as

$$\sigma_{th} = \frac{K_{th,d} + (K_{th,LC} - K_{th,d})(1 - e^{-k(l-d)})}{Y\sqrt{\pi(D+l)}} \quad \text{at } l \geq d, \quad (11)$$

where

$$K_{th,d} = \sigma_{-1,e} Y_1 \sqrt{\pi d}, \quad (12)$$

$$K_{th,LC} = \sigma_{-1,e} Y_2 \sqrt{\pi l_s} = K_{th,d} \frac{Y_2}{Y_1} \sqrt{\frac{l_s}{d}}, \quad (13)$$

$$k = \frac{K_{th,d}}{l_c (K_{th,LC} - K_{th,d})} = \left[l_c \left(\frac{Y_2}{Y_1} \sqrt{\frac{l_s}{d}} - 1 \right) \right]^{-1}. \quad (14)$$

With (12)–(14), Eq. (11) takes on the form

$$\sigma_{th} = \sigma_{-1,e} Y_1 \sqrt{\pi d} \frac{1 + \left(\frac{Y_2}{Y_1} \sqrt{\frac{l_s}{d}} - 1 \right) \left\{ 1 - \exp \left[(d-l) / \left(\left(\frac{Y_2}{Y_1} \sqrt{\frac{l_s}{d}} - 1 \right) l_c \right) \right] \right\}}{Y\sqrt{\pi(D+l)}} \quad \text{at } l \geq d, \quad (15)$$

where Y_1 is the geometrical factor for MSC single grain d deep, $0.67 \leq Y_1 \leq 0.73$ against M [7]

$$Y_1 = Y_2 (2\sqrt{1/(d/l_s + 1)} - 1), \quad (16)$$

Y_2 is the geometrical factor for LC, $Y_2 = 0.73$ [16], Y is the geometrical factor for the notch+crack $D+l$.

The parameter l_s similar to l_D from Eq. (2) is calculated by the formula [11]:

$$l_s = \frac{8^2 \pi (1 + \nu)^2 h}{12 M^2 b} d, \quad (17)$$

where ν is Poisson's ratio, b is the Burgers vector module, M is the Taylor factor, and h is the spacing between neighboring parallel slip planes in the crystal lattice depending on a slip system activated in accordance with the

Taylor factor value. As was shown [11, 15], the parameter l_s characterizes the depth of a surface half-penny PSC on the change of its propagation mechanism in smooth specimens at the uniaxial tensile stress level that exceeds the endurance limit by an infinitesimal. On the other side, it characterizes this depth at which a maximum closure level near its tip is reached that corresponds to the LC closure level at the motive force equivalent to $\Delta K_{th,LC}$. That is, the parameter l_D from Eq. (2), which in the general case Y is a fictitious value, at $Y = Y_2$ acquires the physical meaning and is the material characteristic l_s , defined by Eq. (17), in contrast to a wide-spread view that the material characteristic is the parameter l_0 since it does not depend on Y and is determined as

$$l_0 = \frac{1}{\pi} \left(\frac{\Delta K_{th,LC}}{\Delta \sigma_e} \right)^2, \quad (18)$$

or, with (2) and (18)

$$l_0 = l_D Y^2. \quad (19)$$

But Eq. (18) is the same Eq. (2), only at $Y = 1$, i.e., for the central through-thickness crack in the infinite plane of unit thickness, perpendicular to the direction of uniaxial tensile stress. Thus, l_0 is also a fictitious value that has no physical meaning.

The parameter l_c can be calculated with the phenomenological relation of the grain size d [7]

$$l_c = E^2 b \{A + B \arctan[(E\sqrt{b/4d} - A)/B]\}^{-2}, \quad (20)$$

where $A = (\sigma_f + \sigma_p)/2$, $B = (\sigma_p - \sigma_f)/\pi$, $\sigma_f \cong ME[2(1+\nu)]^{-1} \cdot 10^{-3}$ is the internal friction stress in the crystal lattice, σ_p is the proportionality limit, and E is the elastic modulus.

As was shown [7], just l_c is the critical distance parameter that characterizes the depth of a surface layer with mechanical properties differing from those of the rest of the material [16] where local plastic strains appear under cyclic loading. While many authors take l_0 or l_D as the parameter of critical distance. But such an assumption is mistaken since these parameters, as was mentioned above, have a different physical meaning. Though in some cases, l_s and l_c values can coincide, but such an agreement is accidental that depends, first of all, on the grain size of the material. Thus, by Eq. (17), for alloys with a hexagonal close-packed crystal lattice $l_s \approx (12-13)d$, for alloys with body-centered and face-centered crystal lattices $l_s \approx (6-8)d$. While l_c for fine-grained (high-strength) materials can equal or exceed l_s , for coarse-grained (plastic) materials l_c cannot even exceed a single grain size. And the absolute l_c value for fine-grained materials is much smaller than for the coarse-grained ones. In other words, the l_s/d ratio does not depend on d , and l_c/d does depend.

The endurance limit under symmetrical cycling of smooth specimens $\sigma_{-1,e}$ is calculated by the formula [7]

$$\sigma_{-1,e} = E\sqrt{b/l_c}. \quad (21)$$

For the symmetrical load cycle, Eqs. (10) and (21) are identical since, as was shown in [17], $\Delta K_{th,eff}$ may be evaluated by the formula

$$\Delta K_{th,eff} = E\sqrt{b}. \quad (22)$$

Along with this, l_c in Eq. (10) is a fictitious value, with the account of Eq. (8), while in Eq. (21) it has a concrete physical meaning, as was mentioned above.

Since the ratio $1 \leq Y_2/Y_1 < 1.09$ is unessential for Eq. (15), it can be neglected, and the final form of the equation for evaluating the threshold stress with (21) would be as follows:

$$\sigma_{th} = E\sqrt{b/l_c} Y_1 \sqrt{d} \frac{1 + (\sqrt{l_s/d} - 1) \{1 - \exp[(d-l)/((\sqrt{l_s/d} - 1)l_c)]\}}{Y\sqrt{D+l}} \quad \text{at } l \geq d \quad (23)$$

or

$$\sigma_{th} = \sigma_{-1,e} / K_f, \quad (24)$$

where K_f is the effective stress concentration factor

$$K_f = \frac{1}{Y_1 \sqrt{d} [1 + (\sqrt{l_s/d} - 1) \{1 - \exp[(d-l)/((\sqrt{l_s/d} - 1)l_c)]\}]} \frac{Y \sqrt{D+l}}{1} \quad \text{at } l \geq d. \quad (25)$$

As is seen from Eqs. (24) and (25), for the evaluation of fatigue strength for sharp-edged and deep notches as well as for blunt and shallow ones, a single approach can also be used with the effective stress intensity factor. The difference is only in the approaches to determining K_f . Moreover, the evaluation by Eq. (23) results in the nominal stress.

For evaluating the fatigue strength at the stress ratio R in terms of the applied stress span ($\Delta\sigma_R$) and in terms of the maximum applied cycle stress ($\sigma_{\max,R}$), the empirical formulae can be applied (e.g., [18]):

$$\Delta\sigma_R = \frac{2\sigma_{-1,e}}{1 + (\sigma_{-1,e}(1+R))/(\sigma_{0.2}(1-R))}, \quad (26)$$

$$\sigma_{\max,R} = \Delta\sigma_R / (1 - R), \quad (27)$$

Then $\sigma_{\max,R}$ is substituted for $\sigma_{-1,e}$ into Eq. (24).

Results and Discussion. The calculations by an advanced model and comparison of the data with experimental ones are based on the results of [2, 12]. In [2], the specimens from SM41B structural carbon steel in the form of a strip 45 mm wide and 4 mm thick with a central through-thickness notch 6 mm long and 0.16 mm radius in the root perpendicular to the loading direction are under investigation. The theoretical stress concentration factor is $K_t = 8.48$. The specimens were tension–compression loaded under symmetrical cycling. The material possesses the ferrite-pearlite microstructure with a 64- μm ferrite grain size and the yield limit $\sigma_{0.2} = 194$ MPa. Thus, for calculations by model (23) with (17), (20), and (21), the following initial data were used: for SM41B steel $E = 2.1 \cdot 10^5$ MPa, $\nu = 0.3$, $\sigma_p \cong 0.8\sigma_{0.2} = 155.2$ MPa, $d = 64 \cdot 10^{-6}$ m, for steels $|\bar{b}| = 2.48 \cdot 10^{-10}$ m [17], then by [15], we have $b = |\bar{b}|(2 - \nu)/2 = 2.108 \cdot 10^{-10}$ m, $M = 2$, i.e., the lowest value is employed (most dangerous case) since data on the texture of the material are absent, $Y_1 = 0.67$ for $M = 2$ [15], $|\bar{b}|/h = 1.414$ for a body-centered crystal lattice [19], so $h = 1.754 \cdot 10^{-10}$ m. Since for a given notch $K_t = 8.48$ is practically within the diagram section independent of K_t (Fig. 1a), it may certainly be treated as a crack. In other words, the distribution of local stresses from the notch root is suggested to be similar to the distribution near the LC tip. This notch can also be considered the edge through-thickness crack of a depth that is two times smaller than the length of a through-thickness notch, i.e., $D = 3$ mm. Then the calculation result by Eq. (23) should be doubled. For such a crack, $Y = 1.12$ [20].

In [12], the specimens from 25CrMo4 structural steel in the form of a $100 \times 20 \times 6$ -mm strip with a narrow sharp-edged through-thickness notch of different depths: 0.813, 2.19, and 5.39 mm were studied. The specimens were loaded in eight-point bending under symmetrical cycling. The material possesses the bainite microstructure and indistinct texture with $d \cong 50 \mu\text{m}$ [21] and the yield limit $\sigma_{0.2} = 512$ MPa [12]. Thus, for calculations, the following initial data are used: $E = 2.16 \cdot 10^5$ MPa, $\nu = 0.3$, $\sigma_p = 0.8\sigma_{0.2} = 410$ MPa, $d = 50 \cdot 10^{-6}$ m, $b = 2.108 \cdot 10^{-10}$ m, $h = 1.754 \cdot 10^{-10}$ m, $M = 2$, $Y_1 = 0.67$, and $Y = 1.12$. So all the initial data necessary for calculations are available.

The boundary curves, calculated by Eq. (23) with (17), (20), and (21), as compared to experimental data on crack sizes that formed from the notch root and did not propagate at several load levels are depicted in Fig. 4.

As is seen, the calculated curves of threshold stresses are in good agreement with experimental results, which corroborates the reliability of the advanced model. The calculation by model (23) results in the conservative

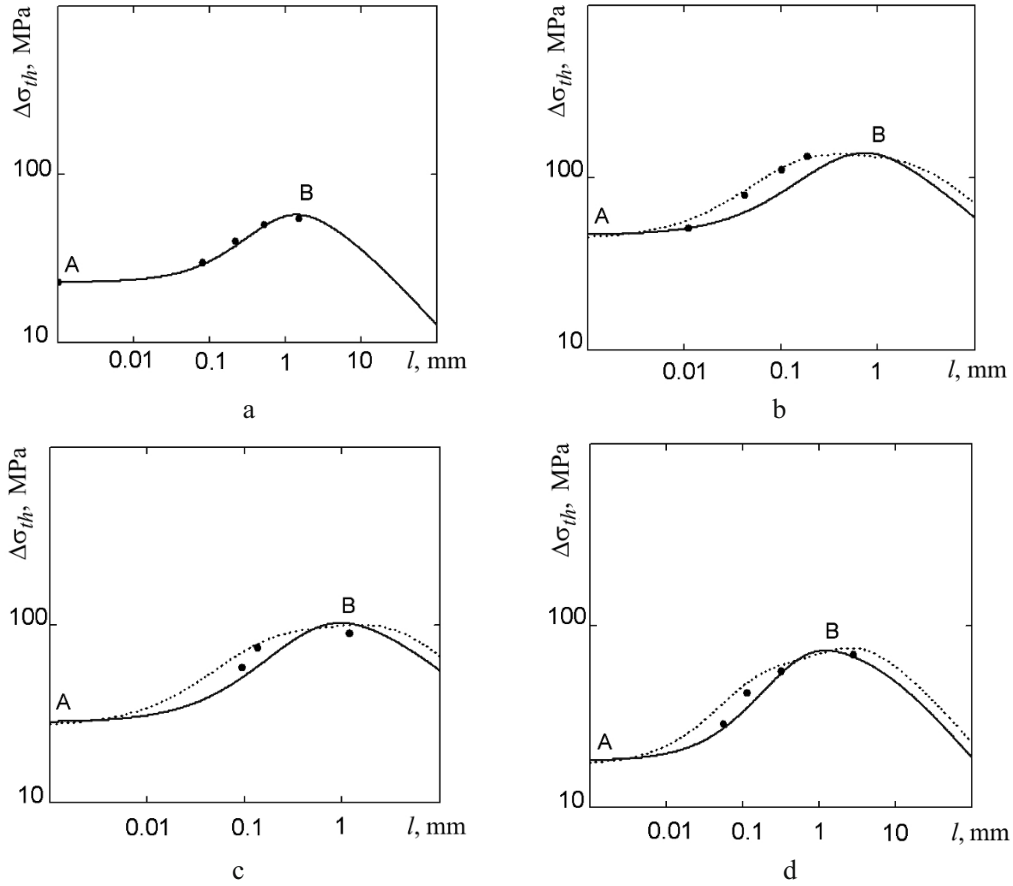


Fig. 4. Comparison of calculated boundary curves (lines) with experimental data (points): (a) SM41B steel specimens, $D=3$ mm; (b, c, d) 25CrMo4 steel specimens, $D=0.813, 2.19,$ and 5.39 mm, respectively. (Solid lines are Eq. (23), broken lines are Eq. (7) [12], A and B are minimum and maximum endurance limits for a given notch, respectively.)

evaluation, while the calculation by Eq. (7) gives a somewhat overstated, i.e., nonconservative one. Moreover, the model does not require long-term and labor-consuming fatigue and fatigue crack resistance tests to get parameters necessary for its implementation. The calculation by model (23) involves only the data on the static strength characteristics E , ν , and σ_p , obtained from short-time tensile tests of standard specimens from an examined material, as well as the microstructure characteristics d , M , b , and h , which are determined from microstructure analysis of the initial material.

The minimum $\sigma_{th,min}$ and maximum $\sigma_{th,max}$ endurance limits for examined notches can also be evaluated by the following simple formulae:

$$\sigma_{th,min} = \Delta K_{th,eff} / (Y \sqrt{\pi D}), \quad (28)$$

$$\sigma_{th,max} = \sigma_{-1,e} / \sqrt{D/l_s + 1}. \quad (29)$$

Equation (28) can offer a determination of the threshold stress necessary for crack initiation from the notch root as LC without the closure of its edges. Formula (29) is the so-called ALM model, modified by the author (l_0/Y^2 is substituted with l_s), for sharp-edged and deep notches, which was obtained in [3] with the KT-diagram. The calculations by these formulae give approximately the same result as by Eq. (23) for the above notches. The calculation by Eq. (28) leads to the totally nonconservative result as compared to (23), the error makes up (+0.3)–(+13.4)%. The calculation by Eq. (29) provides the conservative result in comparison with Eq. (23), the error equals

–1.9 (Fig. 4a), –3.8 (Fig. 4b), –11.2 (Fig. 4c), and –16.3% (Fig. 4d). Thus, the calculated data are even more conservative than the experimental ones. While the advantage of Eq. (23), in addition to the conservative prediction in comparison with experimental data, offers a means of determining arrested crack sizes, which is consistent with the calculated threshold stress.

CONCLUSIONS

1. The advanced model for fatigue strength evaluation permits of calculating the boundary curve of threshold stress spans and corresponding admissible fatigue crack sizes for specimens and structure elements with sharp-edged stress notches ($K_t > 4$) or defects of any depth.

2. The model does not require long-term and labor-consuming fatigue and fatigue crack resistance tests to get parameters necessary for its implementation. The calculation by model (23) involves only the data on the static strength characteristics E , ν , and σ_p , obtained in short-time tensile tests of standard specimens from an examined material, as well as the microstructure characteristics d , M , b , and h , which are determined from microstructure analysis of the initial material.

3. The model reliability was verified with the experimental results for SM41B and 25CrMo4 structural steels taken from the literature, and the data are in good agreement.

4. The practical value of the model lies in prediction of arrested crack sizes at a certain stress span, which is of prime importance for the assessment of the service life of structure elements after the concept of admissible damage.

REFERENCES

1. P. Lukáš and M. Klesnil, "Fatigue limit of notched bodies," *Mater. Sci. Eng.*, **34**, No. 1, 61–66 (1978).
2. K. Tanaka and Y. Akiniwa, "Resistance-curve method for predicting propagation threshold of short fatigue cracks at notches," *Eng. Fract. Mech.*, **30**, No. 6, 863–876 (1988).
3. B. Atzori, P. Lazzarin, and G. Meneghetti, "Fracture mechanics and notch sensitivity," *Fatigue Fract. Eng. Mater. Struct.*, **26**, No. 3, 257–267 (2003).
4. M. Ciavarella and G. Meneghetti, "On fatigue limit in the presence of notches: classical vs. recent unified formulations," *Int. J. Fatigue*, **26**, No. 3, 289–298 (2004).
5. J. C. Ting and F. V. Lawrence, Jr., "A crack closure model for predicting the threshold stresses of notches," *Fatigue Fract. Eng. Mater. Struct.*, **16**, No. 1, 93–114 (1993).
6. K. Sadananda, S. Sarkar, D. Kujawski, and A. K. Vasudevan, "A two-parameter analysis of $S-N$ fatigue life using $\Delta\sigma$ and σ_{\max} ," *Int. J. Fatigue*, **31**, Nos. 11–12, 1648–1659 (2009).
7. O. M. Herasymchuk, O. V. Kononuchenko, and V. I. Bondarchuk, "Fatigue life calculation for titanium alloys considering the influence of microstructure and manufacturing defects," *Int. J. Fatigue*, **81**, 257–264 (2015).
8. M. D. Chapetti, "Fatigue propagation threshold of short cracks under constant amplitude loading," *Int. J. Fatigue*, **25**, No. 12, 1319–1326 (2003).
9. H. Kitagawa and S. Takahashi, "Applicability of fracture mechanics to very small cracks or the cracks in the early stage," in: Proc. of the Second Int. Conf. of Mechanical Behavior of Materials, ASM, Metals Park, OH (1976), pp. 627–631.
10. M. H. El Haddad, T. H. Topper, and K. N. Smith, "Prediction of nonpropagating cracks," *Eng. Fract. Mech.*, **11**, No. 3, 573–584 (1979).
11. O. M. Herasymchuk, "Relationship between the threshold stress intensity factor ranges of the material and the transition from short to long fatigue crack," *Strength Mater.*, **46**, No. 3, 360–374 (2014).
12. J. Maierhofer, H.-P. Gänser, and R. Pippan, "Modified Kitagawa–Takahashi diagram accounting for finite notch depths," *Int. J. Fatigue*, **70**, 503–509 (2015).

13. A. J. McEvily, M. Endo, and Y. Murakami, "On the \sqrt{area} relationship and the short fatigue threshold," *Fatigue Fract. Eng. Mater. Struct.*, **26**, No. 3, 269–278 (2003).
14. O. M. Herasymchuk, O. V. Kononuchenko, P. E. Markovsky, and V. I. Bondarchuk, "Calculating the fatigue life of smooth specimens of two-phase titanium alloys subject to symmetric uniaxial cyclic load of constant amplitude," *Int. J. Fatigue*, **83**, Part 2, 313–322 (2016).
15. O. M. Herasymchuk, "Microstructurally-dependent model for predicting the kinetics of physically small and long fatigue crack growth," *Int. J. Fatigue*, **81**, 148–161 (2015).
16. O. P. Ostash and V. V. Panasyuk, "Fatigue process zone at notches," *Int. J. Fatigue*, **23**, No. 7, 627–636 (2001).
17. R. W. Hertzberg, "A simple calculation of $da/dN - \Delta K$ data in the near threshold regime and above," *Int. J. Fracture*, **64**, R53–R58 (1993).
18. Oleh Herasymchuk and Olena Herasymchuk, "Theoretical estimation of fatigue life under regular cyclic loading," *Mech. Adv. Technol.*, **79**, No. 1, 49–56 (2017).
19. K. S. Chan, "Variability of large-crack fatigue-crack-growth thresholds in structural alloys," *Metall. Mater. Trans. A*, **35**, No. 12, 3721–3735 (2004).
20. Y. Murakami (Ed.), *Stress Intensity Factors Handbook*, in 2 volumes, Vol. 1, Pergamon Press, Oxford (1987).
21. Y. Huo, J. Lin, Q. Bai, et al., "Prediction of microstructure and ductile damage of a high-speed railway axle steel during cross wedge rolling," *J. Mater. Process. Tech.*, **239**, 359–369 (2017).